Direct estimates of reef fish abundance across an artificial reef network

Sean P. Powers [a], **J. Marcus Drymon** [b,c], **Crystal L. Hightower**[a], **Liese M. Carleton**[d], and **John M. Hoenig**[d]

[a]School of Marine and Environmental Sciences, University of South Alabama and the Dauphin Island Sea Lab, 101 Bienville Blvd., Dauphin Island, AL 36528, USA; [b]Coastal Research and Extension Center, Mississippi State University, 1815 Popps Ferry Road, Biloxi, MS 39532, USA; [c]Mississippi-Alabama Sea Grant Consortium, 703 East Beach Drive, Ocean Springs, MS 39564, USA; [d]Virginia Institute of Marine Science, William & Mary, P.O. Box 1346, Gloucester Point, VA 23062, USA

Corresponding author: **Sean P. Powers** (email: spowers@disl.org)

Abstract

Fisheries-independent surveys are commonly used to create indices of relative abundance. If properly designed and calibrated, these surveys may also be used to estimate absolute abundance. Here, we demonstrate the efficacy of this approach by estimating the absolute abundance of red lionfish (*Pterois volitans*), gray triggerfish (*Balistes capriscus*), and red snapper (*Lutjanus campechanus*) across an extensive network of artificial reefs using camera counts, indices of relative abundance, calibration factors, and index-removal estimators. From 2012 to 2017, per reef estimates increased for red lionfish (20×), gray triggerfish (2.1×), and red snapper (2.2×). Network-wide absolute abundances were calculated by multiplying the average per reef estimate by the estimated number of reefs in the network. All increases were consistent with predictions of stock assessment (red snapper), management actions (gray triggerfish), or invasive species colonization (red lionfish). Our methodology demonstrates how estimates of absolute abundance can be derived from fishery-independent surveys and used to evaluate the outputs of stock assessments both in direction and magnitude and quantify critical ecosystem components.

Key words: red snapper, gray triggerfish, red lionfish, artificial reefs, absolute abundance estimate

Introduction

A routine, but often ignored, recommendation from the stock assessments of many fish species is the call for expanded fisheries-independent data collection. Such surveys not only provide data to establish indices of relative abundance, but also contribute to the assessment of growth, age composition, and sexual maturity. For many species, fisheries-independent indices of relative abundance can be of significant value for "tuning" stock assessments. As stock assessment models become increasingly complex, estimates of absolute abundance over defined areas can serve to validate model assumptions as well as provide independent assessments of stock abundance on regional scales. The recommendation to expand fisheries-independent data sources must be balanced with the cost of such expansion (Hansen and Jones 2008) and the potential of such surveys to provide advice to the management process. Fisheries-independent surveys that utilize gear types with broad selectivity both in terms of species and size ranges (e.g., video-based gear, bottom trawls) that can be used in multiple habitats are likely to have greater cost-benefit ratios. Here, we explore an expansion of fisheries-independent surveys to track a group of important reef fish with the added benefit of deriving absolute abundance estimates. In addition to improving current single-species stock assessments, expansion

of fisheries-independent surveys that can provide absolute abundance estimates can provide critical information to advance ecosystem-based management (e.g., generating standing stock biomass estimates of key species for ecosystem models and documenting the colonization and spread of invasive species).

Artificial reef ecosystems provide an appropriate and tractable system in which to apply direct estimation approaches to complement traditional stock assessments and to provide more spatially explicit abundance information (e.g. Szedlmayer et al. 2019; Osowski and Szedlmayer 2022). Globally, artificial reefs (structures deposited on the sea floor with the intent of attracting or enhancing local marine resources) have been deployed for a variety of reasons (Seaman 2000) but most commonly to enhance fishing opportunities for commercial and recreational anglers (Powers et al. 2003; Smith et al. 2016). In many areas fishing effort directed at artificial structures (artificial reefs and petroleum platforms) can account for most harvest. Hence, understanding the portion of the exploitable stock that occupies this habitat type is critical. In the Gulf of Mexico, while densities of fish are high around artificial habitats, most of the stock is in other habitats that cover substantially larger areas (natural hard bottom and unconsolidated sand/mud bottom). Abundance indices that track trends in fish abundance in heavily

exploited habitats are critical to guard against localized depletion or growth overfishing for the portion of the stock that stakeholders utilize the most. If the same gear types used in such surveys can give quantitative estimates of absolute abundance then the exact proportion of the stock size experiencing higher fishing rates can be determined. Such habitat-specific estimates are important component of ecosystem-based management approaches for species that have ontogenetic shifts in habitat requirements (Powers et al. 2018).

In the Gulf of Mexico, artificial reefs provide habitat for several economically important species, red snapper (*Lutjanus campechanus*), gray snapper (*Lutjanus griseus*), gag (*Mycteroperca microlepis*), vermilion snapper (*Rhomboplites aurorubens*), gray triggerfish (*Balistes capriscus*), and greater amberjack (*Seriola dumerili*), many of which are stocks of significant concerns. Of particular interest to the angler community in the northern Gulf of Mexico is the management of red snapper. The fishery is comprised of commercial and recreational sectors which split the annual catch limit (51%:49%, respectively). Alabama coastal waters, which represent just 4% of the U.S. Gulf Coast, account for nearly 30% of the Gulf-wide recreational harvest of red snapper (SEDAR 2017). The commercial fishery off Alabama accounts for 7% of Gulf-wide landings and is regulated under an individual fishing quota system that results in a yearlong fishery.

After decades of overfishing, the red snapper stock was recently classified as not experiencing overfishing and no longer overfished (SEDAR 2013, 2017). The stock is projected to be rebuilt to a Gulf-wide spawning potential ratio (see Goodyear 1993) of 26% by 2032. As the stock rebuilds, anglers have seen increases in catch, as well as the average size, of red snapper. Regulatory changes to guard against a return to overfishing resulted in shortened season lengths during rebuilding (e.g., 9–11 days in some years) for the fishery in federal waters. The contradiction perceived by anglers between the highest catch and yield in recent memory and ever shortening seasons has caused many anglers and policymakers to question the outcome of stock assessments and recent management actions (Powers and Anson 2016, 2019). Other species that are common in artificial reefs, gag, gray triggerfish, and greater amberjack are under aggressive rebuilding programs to end overfishing and rebuild stocks to levels above their long-term biomass targets.

Estimates of fish abundance based on fisheries-independent sampling offer an opportunity to use empirical results to evaluate model assumptions, parameters, and pragmatism and provide stakeholders with easy-to-understand metrics of population size. In addition, abundance estimates based on direct sampling offer a method to assess abundance at smaller geographic scales than most modeling frameworks allow. For many reef fishes, estimating their abundance is made easier given these species' high affinity for structured habitats (Karnauskas et al. 2017). Using several years of data, we estimated the number of artificial reefs across a vast reef network in the northern Gulf of Mexico so that we might apply our abundance estimators to three species along a continuum of demonstrated movement: the relatively mobile red snapper, the less mobile gray triggerfish, and the nearly sedentary invasive red lionfish.

Material and methods

Study site

Networks of artificial and natural hard bottom reefs scattered across otherwise unstructured soft-bottom sediments are typical of many areas of the northern Gulf of Mexico. The largest network of these artificial reefs is the Alabama Artificial Reef Zone (AARZ), a 2668 km^2 area made up of five regions that are pre-permitted by the U.S. Army Corps of Engineers for deposition of artificial reef structures (Fig. 1). Reef placement occurs either by the Alabama Department of Conservation and Natural Resources, Marine Resource Division (MRD) or by private entities. The locations of reefs deployed by MRD are published with coordinates publicly available, while the locations of reefs deployed by private entities are not publicly available. Although a permit ($25) is required to place reefs in the AARZ, many reefs were deployed before the permit requirement and many continue to be deployed without permits. Hence, the exact number of artificial reefs in the zone is unknown.

For our study, the area within the AARZ was divided into 748, 2 × 2 km grids. Beginning in 2011, a subset of these grids was randomly selected each year and surveyed with side-scan sonar prior to sampling using both vertical longlines (VLL) and ROV equipped with video recorders. Grid selection was allocated to three depth strata with the allocation proportional to the bottom area included by each depth. Specifically, 50% of grids selected were in the shallow stratum (18–37 m), 33% in the mid-depth stratum (37–55 m), and 17% in the deep stratum (55–91 m) (described in Gregalis et al. 2012; Powers et al. 2018). From here on, we describe the procedures used for a stratum. Final results were obtained by summing estimates and variances across strata.

Habitat assessment

Side-scan sonar was used to quantify habitat types across the survey area and identify structured habitat locations. A total of 183 selected grids (24% of the AARZ) was surveyed from 2011 to 2017 (Table 1). From 2011 to 2015, each grid was surveyed using an EdgeTech 4200 dual frequency side-scan sonar (300/600 kHz) and a Biosonic echosounder with a 200 kHz single beam transducer. The side-scan towfish was deployed using a data-conducting winch equipped with a digital metering block from the A-frame of the survey vessel and towed at an altitude of approximately 15 m above the seafloor. From 2016 to 2017, grids were surveyed with a pole-mounted EdgeTech 6205 multiphase echosounder (230/550 kHz). Side-scan surveys were typically conducted 4–8 months prior to the reef fish surveys to provide time for data processing. Position, side-scan sonar, and cable-out data were recorded and integrated using Chesapeake Technology Inc. Sonarwiz7 software. This software produced a real-time, fully georeferenced mosaic of the side-scan sonar data and served as a navigational aid for the vessel during the survey. Bottom

Can. J. Fish. Aquat. Sci. **80**: 676–689 (2023) | dx.doi.org/10.1139/cjfas-2022-0094

677

Fig. 1. Location of the Alabama Artificial Reef Zone (AARZ) in the northern Gulf of Mexico. Sampling grids are denoted by filled squares with colors corresponding to the year surveyed. Shading indicates depth zone strata with light gray denoting shallow, gray denoting moderate, and dark gray indicating deep. Depth strata pulled from the USGS' Coastal and Marine Geoscience Data System. Northern Gulf of Mexico shaded relief image at CRM_Hillshade.TIF (https://cmgds.marine.usgs.gov/ publications/of2005-1071/data/background/ngdc/crm_hillshademeta.htm). Reef Permitting Zones from the Alabama Division of Marine Resources (https://www.outdooralabama.com/saltwater-fishing/artificial-reefs).
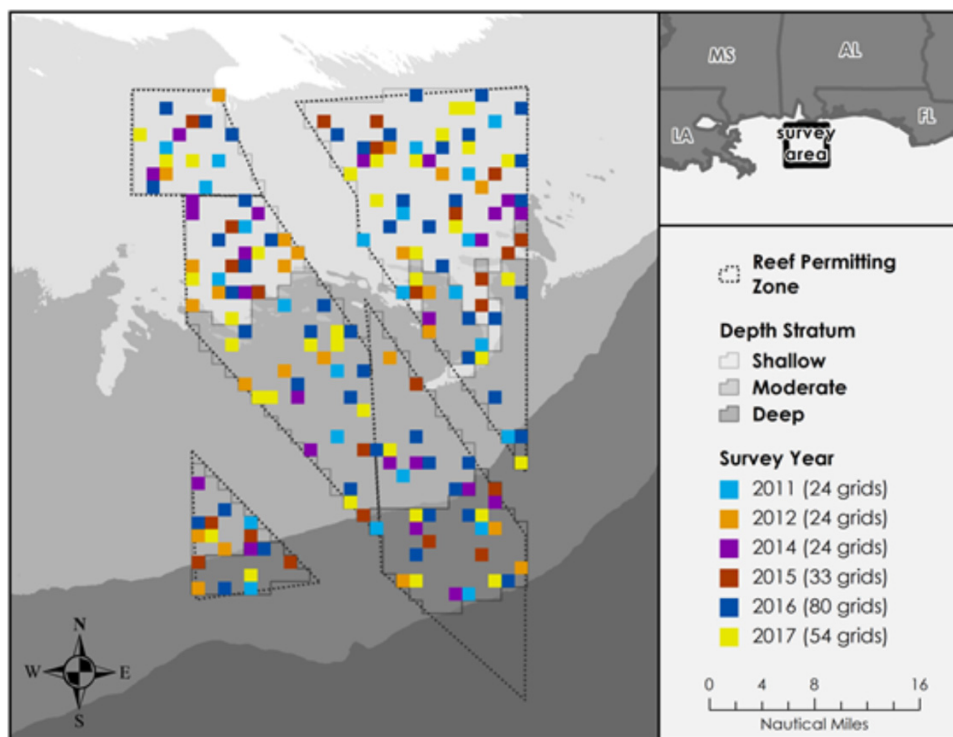
targets visualized by the Sonarwiz7 program were captured and displayed on the chart plotter of the program.

Based on the side-scan generated map of structures, a contact report was produced in which the length, width, height, description, latitude, and longitude of each contact (i.e., each structure) within each grid is marked. These structures were categorized as either a "qualifying structure" (>4 m^2 area and >0.5 m vertical relief) or a "non-qualifying structure" (<4 m^2 area or <0.5 m vertical relief) following Gregalis et al. (2012).

To estimate the number of artificial reefs in the AARZ, we used the information in the contact reports of each grid to determine the number of reefs in each sampling grid. After we enumerated the number of qualifying structures in each grid surveyed (a_i), we computed $\bar{a}$, the average number of artificial reefs per sampled grid in the n grid cells surveyed by

$$(1) \quad \bar{a} = \sum_{i=1}^{n} a_i/n$$

and $\widehat{V}(\bar{a})$, the estimated variance of the mean number of artificial reefs per grid, as

$$(2) \quad \widehat{V}(\bar{a}) = \frac{\sum_{i=1}^{n}(a_i - \bar{a})^2}{n(n-1)}\left(1 - \frac{n}{N}\right)$$

The term $\left(1 - \frac{n}{N}\right)$ is the finite population correction which causes the estimated variance of the estimated mean to go to zero as one approaches a census of all grid cells. Next, we estimated the number of artificial reefs (A) by multiplying this average by the total number of grid cells in the stratum (N). Thus,

$$(3) \quad \widehat{A} = N\bar{a}$$

where the $\wedge$ symbol denotes an estimate. Estimated variance $\left(\widehat{V}\left(\widehat{A}\right)\right)$ of the number of artificial reefs was calculated by

$$(4) \quad \widehat{V}\left(\widehat{A}\right) = N^2\widehat{V}(\bar{a})$$

with standard error of $\widehat{A}$ equal to the square root of $\widehat{V}\left(\widehat{A}\right)$.

Sampling gear for fish

Fish sampling commenced in 2012 with two kinds of sampling gear: a ROV equipped with a video camera and VLL with three hook sizes (see below). It is important to recognize that these two gear types sample different populations as evidenced by the different size compositions of the sampled fish. The VLL sample a narrower range of sizes of fish than is seen by the ROV. Herein, we compute estimates of the size of

Table 1. Summary of sampling effort expressed as the number of randomly chosen grids and randomly chosen stations (in parentheses) by year and survey method.

Survey method	2011	2012	2013	2014	2015	2016	2017
Side-scan sonar	24	24		24	25	50	36
Vertical longline		22 (59)	33 (58)	21 (44)	23 (102)	43 (97)	53 (112)
ROV camera		21 (30)	26 (26)	20 (36)	21 (91)	60 (84)	33 (54)

the population susceptible to sampling by the ROV, i.e., the population potentially seen by the ROV.

Gear 1: remotely operated video

From 2012 to 2017, video images of the fish community at each site selected for ROV surveys were recorded using a high-definition SeaBotix five thruster LBV-300 ROV (2012–2013) and a four thruster Outland 2000 ROV (2014–2017). These ROV-based video surveys were conducted at a subset of sites where VLL collections were performed (Table 1). The ROVs were both equipped with a high-definition, 1080-line, color camera. The ROVs were also equipped with a sonar with a 75 m detection range and 360° viewing capabilities allowing the operator to approach large structures. The ROVs maneuver at approximately 0.25 m·s⁻¹ and 3–4 m from the bottom. The ROV umbilical (250 m) was attached to a 10 kg depression weight, used to reduce the umbilical's catenary. The terminus of the depression weight was maintained 5–10 m from the seafloor, followed by 50 m of unweighted umbilical cord suspended with low buoyancy floats. For each site, the ROV was positioned 5–7 m away from the structure and the cameras pointed at the structure. Five minutes of video was recorded. The process was repeated on the separate side of the structure. Video imagery from the ROV was recorded in HD and analyzed in the laboratory. Fish recorded by the ROV were identified to the lowest possible taxa, enumerated, and measured (see below). For highly mobile fish (e.g., red snapper), abundance was estimated using the MaxN method, wherein the still frame with the most fish visible represents the minimum number of fish present in the sampled area (Schobernd et al. 2013). The still frame used for the maxN count is the frame across any of the two angles that has the highest number of that species in view. This method produced an index of relative abundance for each species on each ROV dive. For species that were slow moving (e.g., gray triggerfish) or near sedentary (red lionfish) total counts of fish on the reef could be made without concern of double counting fish. For these species, this method produced an estimate of absolute abundance per reef. Measurements (total length, TL) of some fish were possible because the ROVs were equipped with a pair of Digi-Key 2.5 milliWatt red lasers aligned in parallel, separated by 3 cm as a frame of reference (Caimi and Tusting 1987). Fish must be nearly perpendicular to the camera and have both lasers illuminate their body to be measured.

Gear 2: vertical longline

Each year from 2012 to 2017, two to four qualifying sites within each grid were randomly selected and designated for

VLL sampling (Table 1). After ROV operations at the site were completed, three VLL were used to collect reef-associated fish. The mainline of the VLL was 167 m of 400 lb (181 kg) test monofilament with a 6/0 Rosco snap swivel crimped onto the end. The backbone was 6.5 m of 300 lb (136 kg) test monofilament. The top of the backbone had a crimped loop to attach the 6/0 Rosco snap swivel from the mainline, and the bottom of the backbone had a 2/0 Rosco snap swivel to attach a 4 kg sash weight. The crimps used at the top and bottom of the backbone were 2.3 mm double copper crimp sleeves. Ten gangions were attached to the backbone described above. Each gangion had a total length of 45.72 cm (18 inches). Gangions were made using a double strand of 100 lb test camouflage monofilament twisted together, terminating in one of three hook sizes: 8/0, 11/0, and 15/0. Each hook size was fished separately on one of the three VLL. All gangions were baited with a piece of Atlantic mackerel (*Scomber scombrus*), cut proportionally to the size of the hook. The VLL was fished for 5 min. After the 5 min soak period, the gear was brought to the surface via a manual crank reel, and the status of each hook recorded (species caught, bait present, or bait absent). All fish were removed from their respective hooks (1–10, shallowest to deepest), and length (standard length, fork length and stretch total length), and weight (kg) recorded. All fish were placed on ice for further processing at the lab. The second and third longlines were fished simultaneously in an identical manner. For complete details of the VLL, see Powers et al. (2018).

Estimates of abundance of model reef fish

To estimate abundance of fish per reef and total abundance in a stratum, we used three methods depending on the mobility of the species and capture probability on hooked gear.

Method 1: direct counts

The first method was applied to red lionfish, which show limited mobility, appearing almost sedentary in video footage but rarely being captured on baited hooks. For the first method, we used the ROV surveys of the reef to count the total number c_{ij} of red lionfish seen on the video at reef j in grid cell i for $i = 1, \ldots, n$ and $j = 1, \ldots m_i$, where n is the number of grid cells surveyed with the video camera and m_i is the number of sites in the ith cell where counts were made. The weighted average total count $\bar{\bar{C}}$ was computed as

$$(5) \quad \bar{\bar{C}} = \frac{\sum_{i=1}^{n} a_i \bar{C}_i}{\sum_{i=1}^{n} a_i}$$

where a_i is the number of reefs in the ith grid cell and $\bar{C}_i$ is the mean of the abundance estimates for the ith grid cell,

$$\bar{C}_i = \frac{\sum_{j=1}^{m_i} c_{ij}}{m_i}.$$

Annual estimates $(\widehat{P}_{\text{tot}})$ of the population in a stratum were obtained by multiplying the average number of fish per reef $\bar{\bar{C}}$ in the stratum by the total number of artificial reefs in the stratum $(\widehat{A})$; thus

(6) $\widehat{P}_{\text{tot}} = \widehat{A}\bar{\bar{C}}$

The total number of red lionfish in the AARZ is estimated by calculating the sum of the three stratum estimates. Variance estimates are given in Appendix A.

Gray triggerfish show very slow movement on video footage and occur in relatively low abundance on reefs (typically <10 fish) allowing enumeration of all fish on the reef via analysis of ROV video footage like that of red lionfish. Hence, we used eqs. 5 and 6 to estimate annual abundance of gray triggerfish as well.

Method 2: calibrating ROV camera counts

The second method was applied to red snapper, a species that demonstrates rapid movements on video footage and can appear in high abundance on artificial reefs (hundreds of fish); consequently, total abundance estimates from video footage are difficult to obtain because of the possibility of double counting or missing some red snapper on a reef. For species like red snapper that are captured easily by hook and line, it is possible to estimate their absolute abundance by using the index-removal method or a calibration factor derived from the index-removal method. This approach involves pairing before and after ROV MaxN counts with the VLL harvest. To establish proof of concept for this approach, separate trials were conducted in 2014 and 2015 where we used ROV surveys (as described earlier) prior to fishing two VLL sets (three lines each deployed two times, six lines total) and then conducted an ROV survey immediately after the two VLL sets. We used the information from these trials to estimate a calibration factor which allow us to estimate total abundance of red snapper from an ROV count (Method 2). For this method to work, the index of population size (ROV count) must be non-selective for size. The removal sample can be fixed in size or variable and there can be size selectivity in the removal process.

Our use of the index-removal approach involves estimating the total population (N) seeable by the ROV along with a camera calibration factor (q_r) from the camera and VLL data from 34 trial sites selected randomly and believed to be representative of the artificial reefs in the AARZ. The calibration factor can then be used to convert camera counts to absolute population size in years or areas where only the ROV is deployed. This approach was used by Eberhardt (1982) for feral horses. The index-removal approach was reviewed by Hoenig and Pollock (1998) and Chen et al. (1998a, 1998b). The ROV de-

ployments provide the two indices of relative abundance, and the VLL provides the removal. This method allows us to convert a change in index into an absolute abundance estimate because we know with certainty the removals over that short time. Given the relatively short time to complete the entire process at a site (~30 min) and the large distance (>0.5 km) between most reef locations, the implicit assumption of no net migration is likely a safe one.

For the estimation of the camera calibration factor (q_r), we let $\bar{C}_1'$ equal the mean of the pre-removal MaxN counts, $\bar{C}_2'$ equal the mean of the post-removal MaxN counts, and $\bar{R}'$ equal the mean of the removals made at the 34 stations. The prime symbol is used to indicate that the catch indices are obtained from an auxiliary study conducted just to estimate the calibration factor q_r. Each station had two VLL sets, and we used the average of the 34 stations to calculate average removal. The expected value of the pre-removal index is assumed to be proportional to the average initial abundance, i.e., $E\left(\bar{C}_1'\right) = q_r \bar{P}$ where $\bar{P}$ is the mean initial abundance/reef and q_r is the calibration coefficient for the ROV camera. Similarly, the expected value of the post-removal index is assumed proportional to the abundance after the removals, i.e., $E\left(\bar{C}_2'\right) = q_r \left(\bar{P} - \bar{R}'\right)$, where $\bar{R}'$ is the mean of the removals over all 34 stations. Then, the average initial abundance (per station) is estimated to be

(7) $\widehat{\bar{P}} = \frac{\bar{R}' \bar{C}_1'}{\bar{C}_1' - \bar{C}_2'}.$

and the catchability of the camera is estimated to be

(8) $\widehat{q}_r = \frac{\bar{C}_1' - \bar{C}_2'}{\bar{R}'}.$

Note that the same sites are visited to obtain the pre-removal and post-removal indices. Chen et al. (1998a) called this the efficient design. In essence, by occupying the same sites for the pre- and post-removal surveys, we induce a positive correlation in the counts that reduces the variance of our estimated catchability. The appropriate equations for computing the variances of $\widehat{P}$ and $\widehat{q}$ are given by Chen et al. (1998a) and detailed in Appendix A.

It may be tempting to estimate q_r separately for each reef, e.g., so variation in catchability can be related to reef-specific factors. However, unless the removal is large relative to the size of the population on a reef, there exists the possibility of obtaining some estimates that are infeasible, e.g., estimated catchability is zero or negative. Averaging the indices and removals across reefs avoids this problem at the cost of assuming catchability is a constant across reefs.

It should be noted that the VLL catch a narrower range of sizes than is seen by the ROV, i.e., the VLL are size-selective (Fig. 2). Despite this, an unbiased estimate of the initial population visible on the ROV is obtained provided the ROV is not size-selective.

In the broader survey of artificial reefs in the AARZ, in which only the ROV is deployed at each site visited and a MaxN count is derived, the total abundance at reef i can be

680

Can. J. Fish. Aquat. Sci. **80**: 676–689 (2023) | dx.doi.org/10.1139/cjfas-2022-0094

Fig. 2. Total lengths (mm) of red snapper captured on vertical longlines ($n = 4876$) or observed on ROV video ($n = 2536$) during surveys of artificial reefs in the Alabama Artificial Reef Zone.
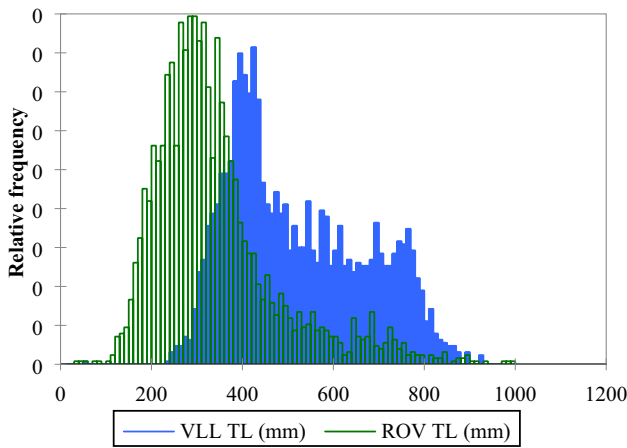
estimated as

$$(9) \quad \widehat{P_i} = \frac{C_i}{\widehat{q}_r}$$

where C_i is the MaxN count on reef i and $\widehat{q}_r$ is the estimated catchability of the camera derived from the 34 before/after trials (eq. 8). The average number of fish per reef in the stratum, $\widehat{P}$, can be estimated as $\widehat{P} = \frac{\bar{\bar{C}}}{\widehat{q}_r}$, while the total number of red snapper can be estimated as

$$(10) \quad \widehat{P}_{\text{tot}} = \frac{\bar{\bar{C}}}{\widehat{q}_r} \widehat{A}$$

where $\widehat{A}$ is the estimated number of artificial reefs in the stratum, $\bar{\bar{C}}$ is the mean MaxN count from all reefs surveyed that year in the stratum, and $\widehat{q}_r$ is as before. The estimated variance of $\widehat{P}$ and $\widehat{P}_{\text{tot}}$ is given in Appendix A.

Method 3: calibrating VLL catches

The third method uses the index-removal method to derive a calibration coefficient for converting the removals data (from the VLL) into estimates of the size of the population potentially seeable by the ROV. For this method to work, the index of population size (ROV count) has to be non-selective for size. The removal gear (VLL) can be size-selective if the calibration factor so derived will be applied to a larger VLL survey of the same population from which the calibration factor is derived. If the calibration factor for the removal gear is to be used to estimate population size for other populations, e.g., other years, those populations must have the same size composition as the population from which the calibration factor is derived if the removal gear is size-selective.

Method 3 is based on the relationship between exploitation rate, u, and population size, P:

$$(11) \quad u = R/P, \text{ thus } P = R/u$$

where R is the VLL removal. We estimate from the study of 34 reefs the exploitation rate u caused by a fixed amount of effort (two VLL sets) as $\widehat{u} = \frac{\bar{C}'_1 - \bar{C}'_2}{\bar{C}'_1}$ (Hoenig and Pollock 1998), where the ^ symbol denotes an estimate (Hoenig and Pollock 1998); the prime symbol is used to indicate that the catch indices (camera counts) are obtained from an auxiliary study conducted just to estimate the calibration factor u. Then we survey a large number of reefs n with VLL; the estimated population size per reef is then $\widehat{P} = \frac{\bar{R}}{\widehat{u}}$, where $\bar{R}$ is the mean removal from the large survey of n reefs, and $\widehat{u}$ is the calibration factor—the estimated exploitation rate—from the separate study of $m = 34$ reefs.

One complication is that in the auxiliary study of the m reefs, two VLL sets were made between the ROV surveys at each site whereas in the large-scale study of n reefs only one VLL set was made. The exploitation rate induced by the removals is related to the fishing effort by $u = 1 - e^{-qf}$, where q is the instantaneous catchability coefficient of the VLL, i.e., the fraction of the population seeable by the ROV camera that is caught by one unit of fishing effort using VLL, and f is the effort. The $f = 2$ sets of VLL give an estimate of exploitation for that level of effort, call it $\widehat{u}_2$. The subscript 2 is to denote that this exploitation rate was achieved with two VLL sets per sampled reef.

In the larger scale survey, one set of VLL was used at each site instead of two. The exploitation rate $\widehat{u}_1$ induced by fishing with $f = 1$ is estimated by noting that $1 - \widehat{u}_2$ is the estimated fraction that survives after two units of fishing effort have been deployed; thus $(1 - \widehat{u}_2)^{.5}$ is the fraction that survives after one unit of fishing effort. The exploitation rate after one unit of fishing effort is thus estimated as

$$(12) \quad \widehat{u}_1 = 1 - (1 - \widehat{u}_2)^{.5} = 1 - \left(1 - \left(\frac{\bar{C}_1 - \bar{C}_2}{\bar{C}_1}\right)\right)^{.5}$$
$$= 1 - \left(\frac{\bar{C}_2}{\bar{C}_1}\right)^{.5}.$$

This is generalized in Appendix A to allow for any level of effort in the auxiliary study and any level of effort in the large-scale survey.

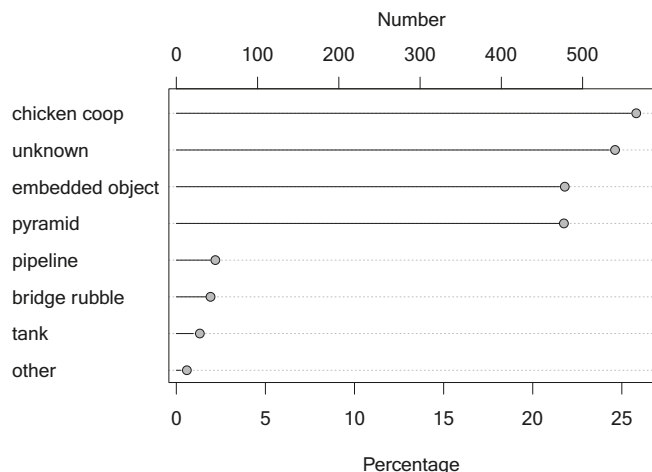The mean population size per reef is then estimated as

$$(13) \quad \widehat{P} = \frac{\bar{R}}{\widehat{u}_1}$$

and the total population is estimated as

$$(14) \quad \widehat{P}tot = \widehat{A} \frac{\bar{R}}{\widehat{u}_1}.$$

The estimated variances for $\widehat{P}, \widehat{P}_{tot}$ and $\widehat{u}_1$ are given in Appendix A.

Fig. 3. Types of artificial reefs detected in the Alabama Artificial Reef Zone based on side-scan sonar survey.

Occupancy model

It may occur that some sites have counts of zero fish of a species for both the camera and VLL gears. It is of interest to know how many of those stations are structural zeros (the site is not suitable habitat so there are no individuals of the species present) and how many are sampling zeros (the site is suitable habitat but any individuals present were missed by both sampling gears). This is estimated using an occupancy model (see Mackenzie et al. 2018) with separate detection parameters for each of the two sampling gears.

The occupancy model assumes the two sampling gears operate independently, each with its own probability of detection. There are three parameters to be estimated: the proportion of the sites that are occupied by the species (i.e., number of sites in which the species is present, whether or not the species is detected), and the conditional probabilities that the species is detected by each of the sampling gears given that the species is present at a site. From these parameters, one can calculate ψ_{condl}, the probability that a site is occupied given that the species is not detected at the site (MacKenzie et al. 2018).

Results

Artificial reef estimation

A total of 183 grids out of a possible 748 grids were chosen randomly and surveyed from 2011 to 2017 (Table 1). Overall, the mean was 9.64 ± 0.368 (one standard error of the mean (SEM)) artificial reefs per grid across all depth strata. By depth stratum, the mean number of artificial reefs per grid was 12.1 ± 0.561 (SEM) in the shallow stratum, 9.08 ± 0.619 (SEM) in mid-depths, and 3.76 ± 0.673 (SEM) in the deeper stratum. The vast majority (>96%) of structures in the shallow and mid-depth strata were classified as artificial structures, with prefabricated pyramids and chicken transport cages the dominant types of artificial structures (Fig. 3). In contrast, structures in the deep stratum were primarily natural relief features (97%) with artificial reefs being rare in

deeper waters. Using the mean number of artificial reefs per grid by stratum, we estimate the total number of artificial structures in the AARZ to be 7213 ± 84.9 (standard error).

Red lionfish

Abundance of red lionfish increased dramatically from 2012 to 2017. The mean counts per reef of red lionfish as observed via ROV video increased from 0.428 ± 0.120 (SEM) per reef in 2012 to a high of 10.3 ± 1.62 (SEM) per reef in 2016 (Table 2). Over the 6-year study, the total number of red lionfish on the estimated 7213 artificial reefs in the AARZ increased from 3085 ± 886 (standard error) in 2012 to a high of 74 150 ± 12 090 (standard error) in 2016 (Fig. 4). The mean TL of the 38 red lionfish measured on the ROV video was 282 ± 8 mm with a minimum size of 190 mm and a maximum size of 356 mm.

Gray triggerfish

Per reef abundance estimates for gray triggerfish based on the ROV video showed an increasing trend over the 6-year period, with the lowest mean count being 1.35 ± 0.261 (SEM) in 2013 and the highest being 2.90 ± 0.428 (SEM) in 2016 (Table 2). Annual estimates of total abundance of gray triggerfish in the AARZ ranged from 9758 ± 1921 (standard error) in 2013 to a high of 20 900 ± 3181 (standard error) in 2016 (Fig. 5). Total length for gray triggerfish measured by the scaling lasers on the ROV (n = 64) averaged 367 mm with a range of 198 to 614 mm.

Red snapper

Red snapper were the most commonly observed reef fish in the video surveys, and the dominant species captured in the VLL surveys. Out of 291 sites that were surveyed with both ROV and VLL, the ROV detected red snapper at 275 sites and the VLL caught red snapper in 234 sites. The occupancy model indicated that there is a 98.3% probability (p_{rov}) of detecting red snapper with the ROV if they are present and an 83.6% probability (p_{vll}) of detecting them with the VLL if they are present. The probability of detecting red snapper with one or both sampling gears, given that they are present, is $p_{rov} + p_{vll} - p_{rov}p_{vll} = 99.72\%$. The probability a site is occupied, given that no red snapper were seen by both gears (what MacKenzie et al. (2018) call ψ_{condl}) is 0.0652. Overall, it is estimated that 280 out of 291 sites were occupied by red snapper and, of the 12 sites where no red snapper were seen, one was occupied by the species (0.0652 × 12 = 0.78 = approximately 1).

The size frequency distribution of red snapper collected by the VLL was shifted to the right compared to the distribution observed by the ROV camera (Fig. 2). From the analysis of ROV video, we recorded sizes of 2536 red snapper with a mean TL of 340 ± 3 (SEM) with a range of 58–990 mm. For the 4876 red snapper captured on the VLL, mean size was 499 ± 2 mm TL with a range of 217–930 mm TL.

Based on the 34 calibration sites from 2014 to 2015, the calibration factor for the red snapper visual survey using the

Table 2. Estimated mean (±SEM) abundance per artificial reef of red lionfish, gray triggerfish, and red snapper for 2012–2017 in the Alabama Artificial Reef Zone.

Species	Method	2012	2013	2014	2015	2016	2017
Red lionfish	1	0.428 ± 0.120	1.6 ± 0.424	3.00 ± 0.906	6.98 ± 1.35	10.3 ± 1.62	6.94 ± 0.855
Gray triggerfish	1	1.42 ± 0.252	1.35 ± 0.261	2.02 ± 0.339	2.25 ± 0.601	2.90 ± 0.428	2.42 ± 0.297
Red snapper	2	75.7 ± 26.7	93.0 ± 36.0	75.0 ± 31.3	107 ± 39.1	139 ± 51.0	158 ± 52.6
Red snapper	3	120 ± 37.3	85.8 ± 27.8	91.6 ± 30.4	67.7 ± 20.3	42.9 ± 14.2	63.9 ± 19.2

Note: Abundance estimates are based on three methods: Method 1: direct counts from ROV; Method 2: calibrating ROV counts; Method 3: calibrating VLL catches. Method 3 is not considered valid (see text) and is presented only to illustrate the importance of meeting the assumptions of the method.

Fig. 4. Estimates of population size by depth stratum in the Alabama Artificial Reef Zone for red lionfish from 2012 to 2017. Solid black line represents the total summed over the three strata, surrounded by one standard error.
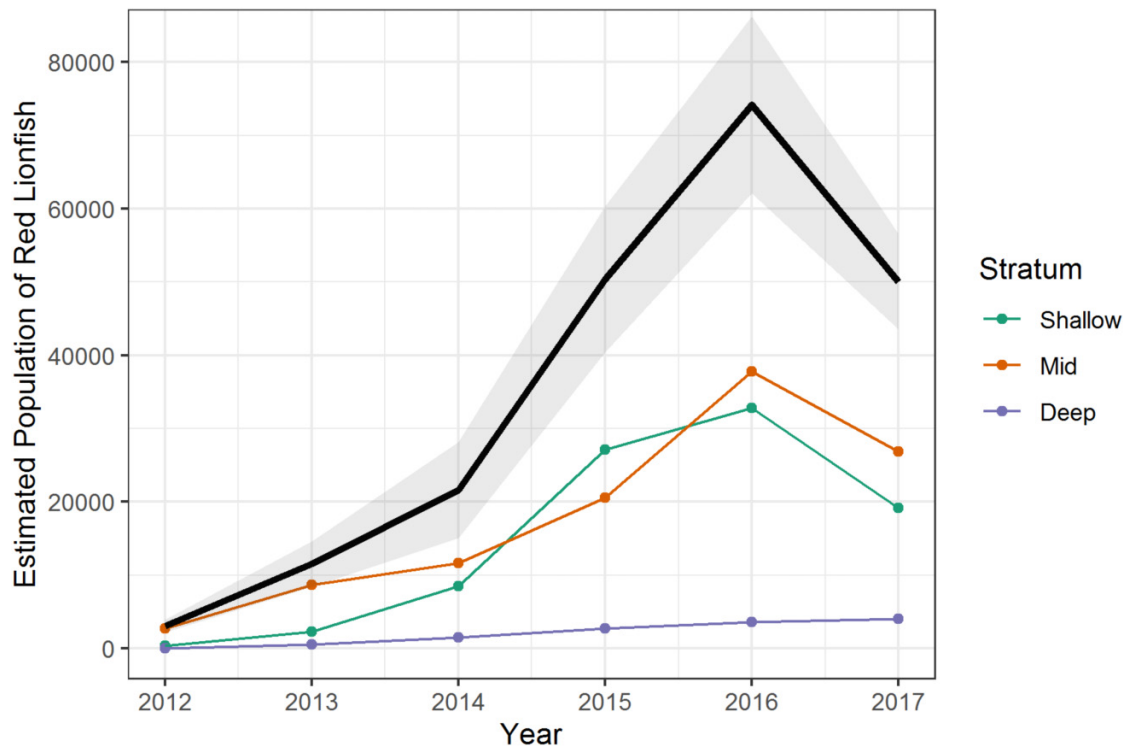
ROV (q_r) was estimated to be 0.119 ± 0.056 (standard error). Similarly, the calibration factor for the vertical line (single unit of fishing effort, u_1) was estimated to be 0.0915 ± 0.040 (standard error).

The two index-removal methods used to calculate red snapper population size showed differing trends (Table 2, Fig. 6). The abundance per reef using the visual survey, as estimated by dividing MaxN by the ROV calibration, showed a generally increasing trend over time. Using this method, the lowest estimated mean population size was in 2014, with 75.0 ± 31.3 (SEM) red snapper per reef. The highest estimated mean population size was in 2017, with 158 ± 52.5 (SEM) red snapper per reef. Conversely, the abundance per reef estimated by dividing the catch per unit effort (CPUE, fish per hook per 5 min) of the vertical line by its calibration factor showed a generally decreasing trend over time. Using this method, the lowest estimated mean population size was in 2016 and the highest in 2012, with 42.9 ± 14.3 (SEM) and 120 ± 37.3 (SEM) red snapper per reef, respectively.

Discussion

This study illustrates the potential of a long-term fisheries-independent survey for providing information beyond calculation of indices of relative abundance and age composition. By combining a survey to determine the extent of habitat, in this case the number of artificial reefs, with an estimate of the average population size per habitat unit (artificial reef), we were able to directly estimate absolute abundance over a discrete area. Notably, our approach provides unbiased estimates of population size and calibration coefficients even if the VLL removal is size-selective, provided the index, (in this case ROV camera) is not size-selective. As more of the AARZ is sampled over time, future estimates of absolute abundance from this region will be more precise.

Assuming the ROV camera is not size-selective, it is possible to obtain a representative sample of fish lengths. While the VLL provides samples that can be aged, the gear is size-selective. However, an unbiased estimate of the age composition in the population can be obtained by applying a

Fig. 5. Estimates of population size by depth stratum in the Alabama Artificial Reef Zone for gray triggerfish from 2012 to 2017. Solid black line represents the total summed over the three strata, surrounded by one standard error.
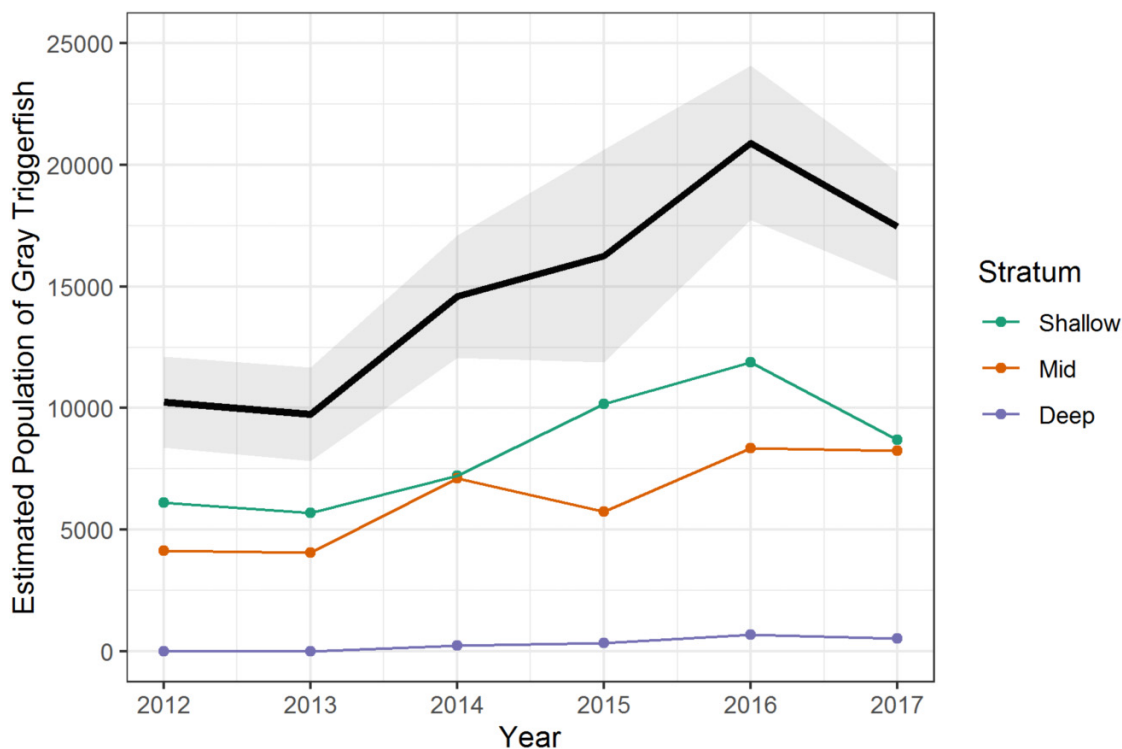

Fig. 6. Total estimated population size of red snapper in the Alabama Artificial Reef Zone from 2012 to 2017. Solid black line represents the total summed over the three strata, surrounded by one standard error. The left plot is estimates produced when using Method 2 (ROV calibration), right is Method 3 (VLL calibration). Method 3 is not considered valid (see text) and is presented just to show the importance of meeting the method's assumptions.
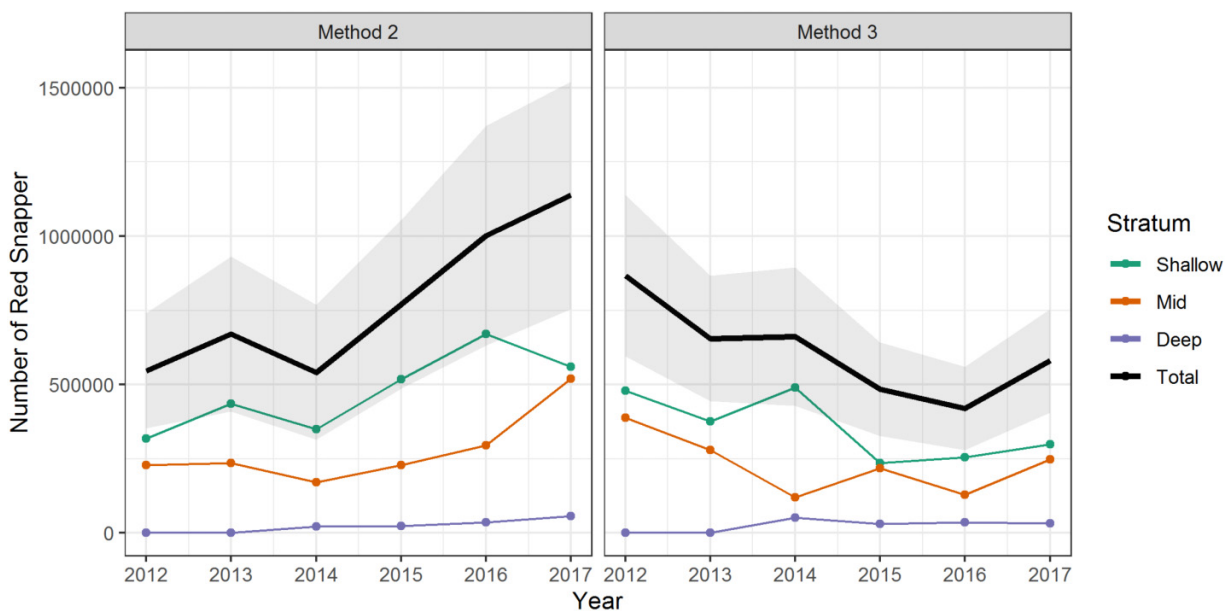
forward (i.e., classic) age-length key derived from the VLL ages to the length frequency distribution obtained from the ROV camera provided the key is obtained in the same year as the length frequencies. If aging is done in only one or a few years, a combined forward-inverse age-length key can be used to estimate the age composition in all (each of the) years (Ailloud and Hoenig 2019). While we did not attempt to do this in this study given limited annual sample sizes, future studies could employ this approach.

Method 1 (direct count from visual survey) was employed to estimate total population size for the species with low mobility, gray triggerfish, and red lionfish. For gray triggerfish, the increase in abundance over time provides a population trajectory for a species with a complicated stock assessment history. Following the completion of SEDAR 43 in 2015, the Gulf of Mexico Fishery Management Council's Science and Statistical Committee concluded that while the assessment was completed using the best available science, the outputs were not useful for providing management advice. Specifically, concerns were raised with respect to declining indices of relative abundance (SEDAR 2015). Preliminary analyses in support of an impending stock assessment indicate small but positive increases in several video-based indices of relative abundance (e.g., Overly and Gardner 2019; Thompson et al. 2019) that are in line with the absolute abundance estimates for gray triggerfish in this study.

Red lionfish showed population trends that were similar to gray triggerfish. While not generated through the stock assessment process, indices of relative abundance for red lionfish have been developed to monitor the spread of this invasive species. Following several years of population expansion in the northern Gulf of Mexico (2012–2016), our absolute abundance estimates indicate a noticeable population decrease in 2017. This trend aligns well with several recent studies (e.g., Campbell et al. 2022) and provides further evidence that the Gulf of Mexico red lionfish invasion may have peaked.

Because estimating absolute abundance of more mobile and abundant fish is more challenging, two potential approaches were examined for estimating absolute abundance of the more mobile red snapper, but in this case only Method 2 (using a calibration factor to convert ROV maxN counts to population size) was deemed appropriate. While both Method 2 and Method 3 provide population estimates of the same order of magnitude, the temporal trends differ for the two approaches. Method 2 indicates an increasing trend over time whereas Method 3 indicates a decreasing trend, suggesting an underlying assumption that one of the methods is flawed. While Methods 2 and 3 are both based on an index-removal estimator relying on the same calibrating index data, the calibration parameters they estimate are for two gears with different selection patterns. Given that Method 3 is parameterized in terms of the ROV camera index, the calibration factor estimated for the VLL would be applicable to the total population seeable by the ROV camera, and not merely to the sub-population that is catchable by the VLL gear. Valid use of Method 2 requires the ROV MaxN counts not depend on the size composition of the fish present while the removals can be size-selective. In contrast, valid use of Method 3 in a given year requires the additional assumption that the gear used for the removals (i.e., VLL) be non-size-selective if the population composition in that year differs from that in the year the calibration factor was derived. That is, there is a subtle assumption that the size composition of fish is the same as when the calibration study was completed, which explains the contrasting trends between the two methods. Consequently, for Method 3 to be used a coefficient would need to be derived each year. The logistics and cost of repeating the calibration experiments through a series of annual index removal experiments would likely be cost prohibitive. In areas where the size composition of the hook and line gear does not show high interannual variability (e.g., given variable fishing pressure for red snapper off coastal Alabama, see Powers and Anson 2019), Method 3 may not require annual repetition of the calibration trials.

Index-removal methods require certain assumptions to be met (Hoenig and Pollock 1998). In the context of the application of the approach to Alabama artificial reefs, key assumptions include the index of abundance being proportional to abundance and the removals being known. The index is the MaxN count from the ROV which has been described by Schobernd et al. (2013). There exists the possibility that the count is influenced by the size of the population. For example, for small structures it might be possible to see almost all of the fish present but for a larger structure, such as an oil platform, there might be a "saturation" effect such that a smaller proportion of the population is seen with increasing size of the structure. For the Alabama artificial reefs in this study, most of the reefs are old chicken coops, small pyramids, or embedded objects (Fig. 3). This minimal variation in size suggests variable catchability due to variation in population size is likely not a problem. The removals data consist of counts of fish brought on board. There exists the possibility that some fish may be hooked and killed but not recovered by the biologists. This happens when fish fall off the hook and die quickly or are otherwise lost to the study. It can also occur if hooked fish are preyed upon, and no carcass is left on the hook to be recovered on haul back of the gear. If there are unaccounted mortalities, this will cause a negative bias in the estimated population size, i.e., from eq. (7) it is seen that an $x\%$ loss of hooked fish causes an $x\%$ underestimate of population size.

A potential problem with the use of calibrated indices to estimate population sizes is missing the target species at some artificial reefs due to low abundance and low sampling effort. That is, reefs where the target species is not detected are assumed to have zero red snapper when in reality they might have been missed at some reefs. This does not appear to be a problem in the current study because red snapper was detected at almost all of the reefs surveyed, and the occupancy model indicates that very few of those sites where no red snapper were seen, were likely to have red snapper present. The incorporation of an occupancy model into the overall study design appears to be prudent because it facilitates evaluation of the model for estimating population sizes.

Fisheries-independent surveys are time consuming, logistically complex, and expensive, all of which create challenges for securing long-term funding. Despite this, the value of these time series for both single and multi-species assessments is unequivocal. As current surveys strive to augment traditional data collections (e.g., otoliths for aging, stomachs for dietary analysis), efforts to estimate absolute abundance for a variety of species should be increasingly considered as a value-added benefit (sensu Link et al. 2008). Periodic estimate of stock-wide absolute abundance can be used to "ground truth" spawning stock biomass estimates of highly parameterized numerical models by providing a check on the

reality of the estimates. Annual estimates may eventually allow for fishery-independent estimates of mortality parameters. While these benefits would come at substantial cost (i.e., expanded sampling and calibration experiments), they would have the added benefit of building public trust in fisheries management. Stakeholders often contrast their on the water, direct observations with the results of stock assessment models. Having an independent data stream of direct observation of abundance from a well-designed study would allow the public to see what management advice is based upon.

Even if stock-wide or annual absolute abundance estimates are not possible (because of fish behavior or logistics and cost), regional or habitat-specific estimates can be used to evaluate the realism of stock assessments. Overall, the temporal trends we detected in our surveys match the predictions of stock assessments that covered the same period or would be anticipated from recent management actions. The most recent terminal year in the Gulf red snapper assessment is 2016 (SEDAR 2017) and the trend is similar to our trend in both direction and rate of increase for the eastern Gulf of Mexico. For gray triggerfish, the most recent stock assessment only covers through 2010 and hence no direct comparison can be made. An assessment was planned with a terminal year of 2018; however, that assessment was halted when questions regarding aging methodology were raised. Consequently, no federal assessment covers this species through our study years. The species is under an aggressive rebuilding program with severely restricted fishing seasons, and hence our trend of increasing abundance is consistent with that action. For red lionfish, a similar pattern of rapid increase followed by stability or moderate decreases have been noted in coastal waters off the panhandle of Florida (Dahl et al. 2019).

Our study demonstrates that rigorously designed fishery-independent surveys that utilize gears with broad selectivity that can be "calibrated" to determine absolute abundance provide significant added value to fisheries-independent surveys. Expansion of such programs could ultimately lead to estimates of absolute abundance of many important fish stocks. On more regional or habitat-specific scales like the one used in our study, regional abundance estimates can be used to detect localized depletions which stock-wide assessments may not detect. The importance of detecting such localized depletions may become more common as more localized and regional management is advanced in response to stakeholder concerns.

Acknowledgements

Article information

Copyright

Data accessibility

Data generated and analyzed during this study are available in the Dauphin Island Sea Lab repository. https://data.disl.edu/dataset/direct-estimates-of-reef-fish-abundance-across-an-artificial-reef-network; it is also available at https://doi.org/10.57778/2dq9-0242

Author information

Author ORCIDs
Sean P. Powers https://orcid.org/0000-0002-4770-9944
J. Marcus Drymon https://orcid.org/0000-0002-2104-004X

Author contribution

Conceptualization: SPP
Data curation: SPP, JMD, CLH, LMC, JH
Formal analysis: SPP, LMC, JH
Funding acquisition: SPP
Investigation: SPP, JMD, CLH, LMC, JH
Methodology: SPP
Project administration: SPP, JMD, CLH
Resources: SPP, JH
Software: SPP, JH
Supervision: SPP, JH
Validation: SPP, LMC, JH
Visualization: SPP, LMC, JH
Writing – original draft: SPP, JH
Writing – review & editing: SPP, JMD, CLH, LMC, JH

Competing interests

Funding

References

Ailloud, L.E., and Hoenig, J.M. 2019. A general theory of age-length keys: combining the forward and inverse keys to estimate age composition from incomplete data. ICES J. Mar. Sci. **76**: 1515–1523. doi:10.1093/icesjms/fsz072.

Caimi, F.M., and Tusting, R.F. 1987. Application of lasers to ocean research and image recording systems. In Proceedings of the International Conference on LASERs 1986, pp. 518–524.

Campbell, M.D., Pollack, A.G., Thompson, K., Switzer, T., Driggers, W.B. Hoffmayer, E.R., et al. 2022. Rapid spatial expansion and population increase of invasive lionfish (*Pterois spp.*) observed on natural habitats in the northern Gulf of Mexico. Biol. Invasions **24**(1): 93–105. doi:10.1007/s10530-021-02625-1.

Chen, C.L., Hoenig, J.M., Dawe, E.G., Brownie, C., and Pollock, K.H. 1998a. New developments in change-in-ratio and index-removal methods, with application to snow crab (*Chionoecetes opilio*). Can. Spl. Pub. Fish. Aquat. Sci. **125**: 49–61.

Chen, C.L., Pollock, K.H., and Hoenig, J.M. 1998b. Combining change-in-ratio, index-removal and removal models for estimating population size. Biometrics, **54**: 815–827. doi:10.2307/2533836.

Cochran, W.G. 1977. Sampling techniques, 3rd ed. John Wiley & Sons, New York.

Dahl, K.A., Edwards, M.A., and Patterson, W.F. 2019. Density-dependent condition and growth of invasive lionfish in the northern Gulf of Mexico. Mar. Ecol.: Progr. Ser. **623**: 145–159. doi:10.3354/meps13028.

Eberhardt, L.L. 1982. Calibrating an index by using removal data. J. Wildl. Manage. **46**: 734–740. doi:10.2307/3808566.

Goodman, L.A. 1960. On the exact variance of products. J. Am. Stat. Assoc. **55**: 708–713. doi:10.1080/01621459.1960.10483369.

Goodyear, C.P. 1993. Spawning stock biomass per recruit in fisheries management: foundation and current use. *In* Risk descriptive evaluation and biological reference points for fisheries management. *Edited by* S.J. Smith, JJ. Hunt and D. Rivard. Can. Spec. Pub. Fish. Aquat. Sci. No. 120. National Research Council of Canada, Ottawa, ON. pp. 67–81.

Gregalis, K.C., Schlenker, L.S., Drymon, J.M., Mareska, J.F., and Powers, S.P. 2012. Evaluating the performance of vertical longlines to survey reef fish populations in the northern Gulf of Mexico. Trans. Am. Fish. Soc. **141**(6): 1453–1464. doi:10.1080/00028487.2012.703154.

Hansen, G.J.A., and Jones, M.L. 2008. The value of information in fishery management. Fisheries, **33**: 340–348. doi:10.1577/1548-8446-33.7.340.

Hoenig, J.M., and Pollock, K.H. 1998. Index-removal methods. *In* Encyclopedia of statistical sciences update: volume 2. *Edited by* S. Kotz, C.B. Read and D.L. Banks. John Wiley and Sons, Inc., New York. pp. 342–346

Karnauskas, M., Walter, J.F., III, Campbell, M.D., Pollack, A.G., Drymon, J.M., and Powers, S.P. 2017. Red snapper distribution on natural habitats and artificial structures in the northern Gulf of Mexico. Mar. Coast. Fish. **9**: 50–67. doi:10.1080/19425120.2016.1255684.

Link, J., Burnett, J., Kostovick, P., and Galbraith, J. 2008. Value-added sampling for fishery independent surveys: don't stop after you're done counting and measuring. Fish. Res. **93**: 229–233. doi:10.1016/j.fishres.2008.04.011.

MacKenzie, D.I., Nichols, J.D., Royle, J.A., Pollock, K.H., Bailey, L.L., and Hines, J.E. 2018. Occupancy estimation and modeling: inferring patterns and dynamics of species occurrence. Elsevier, Amsterdam.

Osowski, A.R., and Szedlmayer, S.T. 2022. Canadian Journal of Fisheries and Aquatic Sciences. **79**(9): 1546–1560. doi:10.1139/cjfas-2021-0227

Overly, K.E., and Gardner, C.L. 2019. Gray triggerfish (*Balistes capriscus*) findings from the NMFS Panama City Laboratory Camera & Trap Fishery-Independent Survey 2004-2017. SEDAR62 WP-06. SEDAR, North Charleston, SC. 32pp.

Powers, S. P., Grabowski, J. H., Peterson, C. H., and Lindberg, W. J. 2003. Estimating enhancement of fish production by offshore artificial reefs: uncertainty exhibited by divergent scenarios. Mar. Ecol. Prog. Ser. **264**: 267–279. doi:10.3354/meps264265.

Powers, S.P., and Anson, K. 2016. Estimating recreational effort in the Gulf of Mexico red snapper fishery using boat ramp cameras: reduction in federal season length does not proportionally reduce catch. N. Am. J. Fish. Manage. **36**: 1156–1166. doi:10.1080/02755947.2016.1198284.

Powers, S.P., and Anson, K. 2019. Compression and relaxation of fishing effort in response to changes in length of fishing seasons for red snapper (*Lutjanus campechanus*) in the northern Gulf of Mexico. Fish. Bull. **117**: 1–7.

Powers, S.P., Drymon, J.M., Hightower, C.L., Spearman, T., Bosarge, G.S., and Jefferson, A. 2018. Distribution and age composition of red snapper (*Lutjanus campechanus*) across the inner continental shelf of the northern Gulf of Mexico. Trans. Am. Fish. Soc. **147**: 791–805. doi:10.1002/tafs.10081.

Schobernd, Z.H., Bacheler, N.M., and Conn, P.B. 2013. Examining the utility of alternative video monitoring metrics for indexing reef fish abundance. Can. J. Fish. Aquat. Sci. **71**: 464–471. doi:10.1139/cjfas-2013-0086.

Seaman, W. S., Jr. 2000. Artificial reef evaluation with application to natural marine habitats. CRC Press, Boca Raton, FL

Seber, G.A.F. 1982. The estimation of animal abundance and related parameters. 2nd ed. Macmillan, New York.

SEDAR (Southeastern Data Assessment and Review). 2013. Gulf of Mexico red snapper stock assessment report (SEDAR 31). SEDAR, North Charleston, SC.

SEDAR (Southeastern Data Assessment and Review). 2015. Gulf of Mexico gray triggerfish stock assessment report (SEDAR 43). SEDAR, North Charleston, SC.

SEDAR (Southeastern Data Assessment and Review). 2017. Gulf of Mexico red snapper stock assessment report (SEDAR 52). SEDAR, North Charleston, SC.

Smith, J.A., Lowry, M.B., Champion, C., and Suthers, I.M. 2016. A designed artificial reef is among the most productive marine fish habitats: new metrics to address 'production versus attraction'. Mar. Biol. **163**: 188. doi:10.1007/s00227-016-2967-y.

Szedlmayer, S.T., Mudrak, P.A., and Jaxion-Harm, J. 2019. A comparison of two fishery-independent surveys of red snapper, *Lutjanus campechanus*, from 1999–2004 and 2011–2015.In Red Snapper biology in a changing world, pp. 249-274. CRC Press. doi:10.1201/9781351242776

Thompson, K.A., Switzer, T.S., Christman, M.C., Keenan, S.F., Gardner., C., Overly, K.E., and Campbell, M. 2019. Indices of abundance for gray triggerfish (*Balistes capriscus*) using combined data from three independent video surveys. SEDAR62-WP-01. SEDAR, North Charleston, SC. 17pp.

Appendix A. Statistical design and estimators for fish per reef and total number of fish A

The AARZ was divided into three strata based on depth. Since strata are, by definition, sampled independently, estimates of totals for the entire AARZ are obtained as the sum over strata of the stratum-specific estimates. The variance of the total is estimated as the sum of the stratum-specific variances. Below, we discuss the procedure for obtaining estimates for a stratum.

Total number of reefs

The total number of reefs (either artificial or natural—the procedure is the same for the two types of reefs) is estimated from a simple random sample of grid cells, each of which is mapped completely. Let the total number of grid cells in a stratum be N, of which n is selected for mapping the reef structures, and let the number of reefs counted in grid cell i be denoted by a_i. The average number of artificial reefs per sampled grid is

(A1) $\quad \bar{a} = \sum_{i=1}^{n} a_i/n$

Can. J. Fish. Aquat. Sci. **80**: 676–689 (2023) | dx.doi.org/10.1139/cjfas-2022-0094

687

with the variance of the mean number of artificial reefs per grid estimated as

(A2) $\quad \widehat{V}(\bar{a}) = \dfrac{\sum_{i=1}^{n}(a_i - \bar{a})^2}{n(n-1)}\left(1 - \dfrac{n}{N}\right)$

The term $\left(1 - \frac{n}{N}\right)$ is the finite population correction, which causes the variance of the estimated mean to go to zero as a census of all grid cells is approached. The estimated number of reefs in the entire stratum $\left(\widehat{A}\right)$ is obtained by multiplying the average number of reefs per cell by the total number of grid cells in the stratum:

(A3) $\quad \widehat{A} = N\bar{a}$

with estimated variance $\left(\widehat{V}\left(\widehat{A}\right)\right)$ given by

(A4) $\quad \widehat{V}\left(\widehat{A}\right) = N^2 \widehat{V}(\bar{a})$

with standard error of $\left(\widehat{A}\right)$ equal to the square root of $\widehat{V}\left(\widehat{A}\right)$.

Method 1: direct counts

For each stratum, two-stage cluster sampling with units of unequal size is used to estimate the mean number of fish per reef. We assume that the camera count at a reef is the abundance at the reef. At the first stage, a random sample of n out of N grid cells is selected. At the second stage, m_i out of a_i reefs are sampled from the ith sampled grid cell, for $i = 1, \dots$ n with $2 \le m_i \le a_i$. The mean number of fish per reef, averaged over reefs within a grid cell and over grid cells, is estimated as (Cochran 1977, p. 305)

(A5) $\quad \bar{\bar{C}} = \dfrac{\sum_{i=1}^{n} a_i \bar{C}_i}{\sum_{i=1}^{n} a_i}$

where $\bar{C}_i$ is the average of the observations of abundance on the m_i reefs observed in grid cell i. The double bar in $\bar{\bar{C}}$ denotes the mean is taken both over observations within grid cells and over grid cells.

The variance of $\bar{\bar{C}}$ is estimated as (see Cochran 1977 p. 305)

(A6) $\quad \widehat{V}\left(\bar{\bar{C}}\right) = \dfrac{N^2}{n\widehat{A}^2}(1 - n/N)\dfrac{\sum_{i=1}^{n} a_i^2\left(\bar{C}_i - \bar{\bar{C}}\right)^2}{n-1}$
$\qquad\qquad + \dfrac{N}{n\widehat{A}^2}\sum_{i=1}^{n}\dfrac{a_i^2(1 - m_i/a_i)\sigma_{2i}^2}{m_i}$

where $1 - n/N$ is the finite population correction at the first stage, $1 - m_i/a_i$, is the finite population correction at the second stage, and

$\sigma_{2i}^2 = \dfrac{\sum_{j=1}^{m_i}\left(c_{ij} - \bar{C}_i\right)^2}{m_i - 1}$

where c_{ij} is the observed abundance at the jth reef observed in the ith grid cell. It may happen that some or all of the grid cells have only one observation per cell. In the former

case, the second stage variance σ_{2i}^2 can be computed using only cells with two or more observations per cell, and the second term of the variance of $\widehat{V}\left(\bar{\bar{C}}\right)$ in eq. (A6) has the number of grid cells sampled, n, replaced with the number of grid cells sampled with $m_i \ge 2$.

The total number of fish (in a stratum), P_{tot}, is estimated as the product of the number of reefs and the number of fish per reef. Thus,

(A7) $\quad \widehat{P}_{\text{tot}} = \widehat{A}\bar{\bar{C}}$

where $\widehat{P}_{tot}$ is the estimated number of fish in the stratum. The unbiased estimate of the variance of this product is (Goodman 1960)

(A8) $\quad \widehat{V}\left(\widehat{P}_{tot}\right) = \widehat{A}^2\widehat{V}\left(\bar{\bar{C}}\right) + \bar{\bar{C}}^2\widehat{V}\left(\widehat{A}\right) - \widehat{V}\left(\bar{\bar{C}}\right)\widehat{V}\left(\widehat{A}\right).$

The estimated variance of $\widehat{A}$ is given by eq. (A4) above. The estimated variance of $\bar{\bar{C}}$ is given by eq. (A6). Note that as the number of grid cells mapped to locate reefs approaches the total number of grid cells, the second and third terms in the above approach 0. That is, they are needed only because the total number of reefs is estimated and not known perfectly.

Method 2: calibrating ROV camera counts

The estimator of the total number of fish on all reefs in a stratum is

(A9) $\quad \widehat{P}_{tot} = \dfrac{\bar{\bar{C}}}{\widehat{q}_r}\widehat{A}$

where the symbols are as defined in the main text. Here, we are assuming that $\widehat{q}_r$ and $\widehat{A}$ are estimated from auxiliary studies and $\bar{\bar{C}}$ is estimated from a current survey. The estimated variance is found by the delta method (Seber 1982, p. 7) to be

(A10) $\quad \widehat{V}\left(\widehat{P}_{\text{tot}}\right) = \left(\dfrac{\partial \widehat{P}_{\text{tot}}}{\partial \bar{\bar{C}}}\right)^2\widehat{V}\left(\bar{\bar{C}}\right) + \left(\dfrac{\partial \widehat{P}_{\text{tot}}}{\partial \widehat{A}}\right)^2\widehat{V}\left(\widehat{A}\right) + \left(\dfrac{\partial \widehat{P}_{\text{tot}}}{\partial \widehat{q}_r}\right)^2\widehat{V}\left(\widehat{q}_r\right)$
$\qquad\qquad = \dfrac{\widehat{A}^2}{\widehat{q}_r^2}\left(\widehat{V}\left(\bar{\bar{C}}\right) + \dfrac{\bar{\bar{C}}^2}{\widehat{A}^2}\widehat{V}\left(\widehat{A}\right) + \dfrac{\bar{\bar{C}}^2}{\widehat{q}^2}\widehat{V}\left(\widehat{q}_r\right)\right).$

Note that the covariances among $\widehat{A}$, $\bar{\bar{C}}$, and $\widehat{q}_r$ are zero since they are estimated independently. The component variances are estimated as follows. The variance of $\widehat{A}$ is estimated from eq. (A4) above. The variance of $\bar{\bar{C}}$ is estimated as for means from two-stage cluster sampling using eq. (A6) above.

The estimate of q_r is

(A11) $\quad \widehat{q}_r = \dfrac{\bar{C}_1' - \bar{C}_2'}{\bar{R}'}$

where $\bar{C}_1'$ and $\bar{C}_2'$ are the mean counts of fish at the m sites before and after the removals, respectively, $\bar{R}'$ is the mean of the removals at the m sites, and the estimated variance of $\widehat{q}_r$

is found using the delta method to be

$$(A12) \quad \widehat{V}(\widehat{q}_r) = \frac{1}{\bar{R}'^2}\left(\widehat{V}(\bar{C}_1') + \widehat{V}(\bar{C}_2') + \frac{(\bar{C}_1' - \bar{C}_2')^2}{\bar{R}'^2}\widehat{V}(\bar{R}') - 2\widehat{Cov}(\bar{C}_1', \bar{C}_2')\right.$$
$$\left. - \frac{2(\bar{C}_1' - \bar{C}_2')}{\bar{R}'}\widehat{Cov}(\bar{C}_1', \bar{R}') + \frac{2(\bar{C}_1' - \bar{C}_2')}{\bar{R}'}\widehat{Cov}(\bar{C}_2', \bar{R}')\right)$$

The three variances in (A12) are calculated in the usual fashion as for the mean from a simple random sample. The three covariances are computed from the paired observations as

$$\widehat{Cov}(\bar{X}, \bar{Y}) = \frac{\sum_{i=1}^{n}(X_i - \bar{X})(Y_i - \bar{Y})}{n(n-1)}$$

The n in the denominator is because we want $\widehat{Cov}(\bar{X}, \bar{Y})$ instead of $\widehat{Cov}(X, Y)$; here X and Y are a pair of parameters from $\{\bar{C}_1, \bar{C}_2, \bar{R}\}$.

The average number of fish per reef, $\bar{P}$, is estimated as

$$(A13) \quad \widehat{\bar{P}} = \frac{\bar{\bar{C}}}{\widehat{\bar{q}}_r}$$

The estimated variance of $\widehat{\bar{P}}$ is obtained from (A10) with $\widehat{A}$ replaced by 1.0 and the term with $\widehat{V}(\widehat{A})$ ignored.

Method 3: calibrating longline catches

The third method is based on the relationship between exploitation rate, u, and population size, P, i.e., $u = R/P$, thus $P = R/u$, where R is the removal. We estimate from an auxiliary study the exploitation rate caused by a fixed amount of longline effort as $\widehat{u} = \frac{\bar{C}_1' - \bar{C}_2'}{\bar{C}_1'}$, where $\bar{C}_1'$ and $\bar{C}_2'$ are the mean camera counts of fish at m sites before and after the removals, respectively. Then we survey a large number of reefs n with VLL; the estimated population size per reef is then $\widehat{\bar{P}} = \frac{\bar{R}}{\widehat{u}}$, where the $\wedge$ symbol denotes an estimate, $\bar{R}$ is the mean removal from the large survey of n reefs, and $\widehat{u}$ is the calibration factor—the estimated exploitation rate—from the separate study of m reefs (=34 in this study). The average removal, $\bar{R}$, can be obtained by any sampling design, e.g., the two-stage sampling of reefs within grid cells used in this paper. The exploitation rate is related to the fishing effort by $u = 1 - e^{-qf}$, where q is the instantaneous catchability coefficient of the VLL and f is the effort. In this study, $f = 2$ sets of VLL were fished at each of the 34 stations, giving an estimate of $\widehat{u}_2$. The subscript 2 is to denote that this exploitation rate was achieved with two VLL sets per sampled reef. For this part of the study, the fieldwork was designed to test index-removal estimation and calibration of sampling gear and representative sites were chosen to test the field procedures. The derived calibration factor was applied to sampling in subsequent years on the assumption that the calibration factor is constant over time and space. Thus, the two-stage cluster sampling design was not followed.

In the larger scale survey, one set of VLL was used at each site instead of two. The exploitation rate induced by fishing with $f = 1$ is estimated by

$$\widehat{u}_1 = 1 - \sqrt{1 - \widehat{u}_2} = 1 - \left(1 - \left(\frac{\bar{C}_1' - \bar{C}_2'}{\bar{C}_1'}\right)\right)^{.5}$$
$$= 1 - \left(\frac{\bar{C}_2'}{\bar{C}_1'}\right)^{.5}$$

More generally, the exploitation rate caused by k units of fishing effort is given by

$$\widehat{u}_k = 1 - \left(1 - \left(\frac{\bar{C}_1' - \bar{C}_2'}{\bar{C}_1'}\right)\right)^{\phi} = 1 - \left(\frac{\bar{C}_2'}{\bar{C}_1'}\right)^{\phi}$$

where ϕ is the ratio of the level of effort used in the auxiliary study divided by the level of effort k used in the large-scale study.

The mean population size per reef, when one VLL set is used per site, is then estimated as

$$\widehat{\bar{P}} = \frac{\bar{R}}{\widehat{u}_1}$$

and the total population is estimated as

$$\widehat{P}_{tot} = \widehat{A}\frac{\bar{R}}{\widehat{u}_1}.$$

The variance of these estimators is obtained using the delta method assuming $\bar{R}$, $\widehat{u}_1$ and $\widehat{A}$ are estimated independently:

$$\widehat{V}(\widehat{\bar{P}}) = \frac{\widehat{V}(\bar{R})}{\widehat{u}_1^2} + \left(\frac{\bar{R}}{\widehat{u}_1^2}\right)^2\widehat{V}(\widehat{u}_1)$$

$$\widehat{V}(\widehat{P}_{tot}) = \left(\frac{\bar{R}}{\widehat{u}_1}\right)^2\widehat{V}(\widehat{A}) + \left(\frac{\widehat{A}}{\widehat{u}_1}\right)^2\widehat{V}(\bar{R}) + \left(\frac{\widehat{A}\bar{R}}{\widehat{u}_1^2}\right)^2\widehat{V}(\widehat{u}_1)$$

The estimated variance of $\widehat{u}_1$ is

$$\widehat{V}(\widehat{u}_1) = \frac{\bar{C}_2'}{4(\bar{C}_1')^3}\widehat{V}(\bar{C}_1') + \frac{1}{4\bar{C}_1'\bar{C}_2'}\widehat{V}(\bar{C}_2')$$
$$- \frac{1}{2(\bar{C}_1')^2}\widehat{Cov}(\bar{C}_1', \bar{C}_2')$$

The variances of $\bar{R}$ and $\widehat{A}$ are estimated according to the sampling design used, e.g., two-stage cluster sampling for $\bar{R}$ (eq. A6 with R substituted for C) and simple random sampling for $\widehat{A}$ (eq. A4).